Homogeneous Catalysis

International Edition: DOI: 10.1002/anie.201504813
German Edition: DOI: 10.1002/ange.201504813

Selective Alcohol Oxidation by a Copper TEMPO Catalyst: Mechanistic Insights by Simultaneously Coupled Operando EPR/UV-Vis/ATR-IR Spectroscopy

Jabor Rabeah, Ursula Bentrup,* Reinhard Stößer, and Angelika Brückner**

Abstract: *The first coupled operando EPR/UV-Vis/ATR-IR spectroscopy setup for mechanistic studies of gas-liquid phase reactions is presented and exemplarily applied to the well-known copper/TEMPO-catalyzed (TEMPO = (2,2,6,6-tetramethylpiperidin-1-yl)oxyl) oxidation of benzyl alcohol. In contrast to previous proposals, no direct redox reaction between TEMPO and Cu^{I}/Cu^{II} has been detected. Instead, the role of TEMPO is postulated to be the stabilization of a (bpy)(NMI)Cu^{II}-$O_2^{\cdot-}$-TEMPO (bpy = 2,2′-bipyridine, NMI = N-methylimidazole) intermediate formed by electron transfer from Cu^{I} to molecular O_2.*

Rational catalyst design requires reliable knowledge on structure–reactivity relationships, which can only be obtained under relevant reaction conditions. Preferentially, simultaneous couplings of suitable spectroscopies in the same experiment should be used, because no single method can provide the whole information needed and coupling ensures identical reaction conditions and optimum comparability of results.[1] For homogeneous metal-catalyzed reactions, coupled UV-Vis/ATR-IR/Raman spectroscopy was shown to be an ideal tool for mechanistic studies, because—in addition to metal ions—organic reaction intermediates can be identified.[2]

In this work, we have for the first time simultaneously coupled operando ATR-IR, UV-Vis, and EPR spectroscopy. To demonstrate the benefits for mechanistic studies, we have revisited the well-known aerobic oxidation of primary alcohols to aldehydes in the presence of $Cu^{I}OTf$ or $Cu^{II}(OTf)_2$ as metal precursors, a 2,2-bipyridine (bpy) ligand, a *N*-methylimidazole (NMI) base and 2,2,6,6-tetramethylpiperidine-1-oxyl (TEMPO) as cocatalyst. Whereas EPR and UV-Vis spectroscopy monitored both paramagnetic (Cu^{2+}, TEMPO) and diamagnetic species (Cu^{+}), ATR-IR spectroscopy detected the catalytic activity by visualizing the alcohol-to-aldehyde conversion. Despite the fact that this reaction has been studied frequently in the past,[3] it is still a challenge to use air as oxidant and different partially contradicting reaction mechanisms were proposed without providing sufficient experimental evidence for the postulated intermediates.

So far the most efficient catalytic system has been developed by the group of Stahl[3a–c,4] who also presented a thorough mechanistic and kinetic study including in situ ATR-IR and UV-Vis data as well as EPR spectra of quenched frozen solutions.[3b] A two-step catalytic cycle has been proposed comprising 1) oxidation of Cu^{I} and TEMPOH by O_2 via a Cu^{II}-(O_2)-Cu^{II} dimer to single Cu^{II} and TEMPO, and 2) oxidation of the alcohol by single Cu^{II} and TEMPO which regenerates Cu^{I} and TEMPOH. Since no TEMPOH is present at the start of the reaction, it was speculated that the alcohol reacts with the Cu^{II}-(O_2)-Cu^{II} dimer, forming Cu^{II}-OOH and Cu^{II}-OCH_2R species. However, as shown below, we could not confirm such a reaction by in situ EPR measurements. Thus, the role of TEMPO remains still unclear. Moreover, no direct evidence for the Cu^{II} dimer was presented. The same mechanism was proposed starting from a Cu^{II} catalyst, whereby it remains an open question how this is reduced to the Cu^{I} starting species in the postulated cycle.

To learn more about these still unclear aspects, we have studied the interaction of the different components in the reaction mixture in a more detailed sequential way. We started with a solution of 0.1 mmol $Cu^{I}OTf$ in acetonitrile (MeCN) which is diamagnetic and does not show any EPR signal, also not after adding 0.1 mmol bpy ligand. The UV-Vis spectrum of $Cu^{I}OTf$ in MeCN at 20 °C shows a sharp metal-to-ligand charge-transfer (MLCT) band at 310 nm (Figure 1 A, a). After adding the bpy ligand, a new MLCT band appears at 450 nm with a shoulder at 530 nm whereas the band at 310 nm is shifted to higher wavelength (348 nm, Figure 1 A, b), indicating the replacement of coordinated solvent molecules at the Cu^{I} site by bpy. Upon subsequent bubbling of O_2 through the solution, the bands at 450 and 530 nm lost intensity and shifted to 443 and 550 nm, respectively (Figure 1 A, c). We attribute these changes to a dipolar interaction of the (bpy)Cu^{I} complex with O_2 rather than to the oxidation of (bpy)Cu^{I} to a tentative EPR-silent (bpy)Cu^{II}-$O_2^{\cdot-}$ monomer or a (bpy)Cu^{II}-O_2-Cu^{II}(bpy) dimer species as postulated in other papers,[5] since light absorption around 660 nm expected for d–d transitions of Cu^{II}[5c] is negligible (Figure 1 A, c). Moreover, the bpy ligand and MeCN are known to stabilize Cu^{I} and render it stable against oxidation.[3b]

When NMI was added to the solution of (bpy)Cu^{I} under O_2 in the next step, the band at 443 nm broadened and disappeared with time while new ligand-to-metal charge-transfer (LMCT) and d–d bands appeared at 345 and 650 nm,

[*] Dr. J. Rabeah, Dr. U. Bentrup, Prof. Dr. A. Brückner
Leibniz-Institut für Katalyse e.V. an der Universität Rostock
Albert-Einstein-Str. 29a, 18059 Rostock (Germany)
E-mail: jabor.rabeah@catalysis.de
ursula.bentrup@catalysis.de
angelika.brueckner@catalysis.de
Prof. Dr. R. Stößer
Institut für Chemie-Humboldt-Universität zu Berlin
Brook-Taylor-Str. 2, 12489 Berlin-Adlershof (Germany)

Supporting information for this article is available on the WWW under http://dx.doi.org/10.1002/anie.201504813.

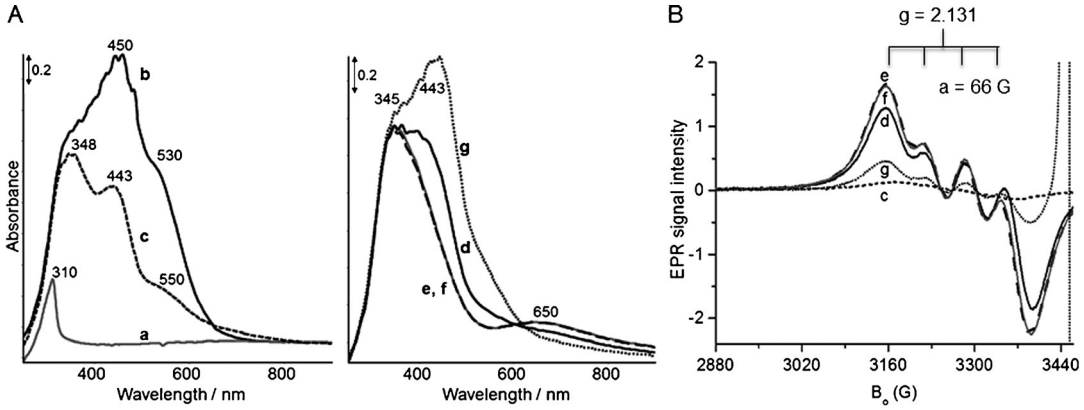

Figure 1. A) Subsequent UV-Vis spectra of complex $[(MeCN)_4]CuOTf$ in MeCN solution (a), + bpy (b), after 20 min bubbling O_2 through this solution at 20 °C (c), + NMI immediately (d), + NMI after 15 min (e), + BzOH (f), + TEMPO (g); B) corresponding EPR spectra in the range of the Cu^{II} signal.

respectively, indicating the oxidation of Cu^{I} to Cu^{II} species (Figure 1 A, d and e). This is also evident from the corresponding EPR spectra (Figure 1 B, d and e), in which a characteristic signal of Cu^{II} species appears. When this sample was measured in frozen solution (−183 °C), the signal became anisotropic, thus confirming the octahedral geometry of the Cu^{II} species (Figure S1).[6] It is very probable that oxidation of Cu^{I} to Cu^{II} goes along with the transfer of one electron from Cu^{I} to O_2 forming an initial (bpy)-(NMI)$Cu^{II}O_2^{\cdot-}$ intermediate which, however, might not be seen by EPR due to magnetic interaction between paramagnetic Cu^{II} and $O_2^{\cdot-}$. On the other hand, $O_2^{\cdot-}$ is known to be very reactive and could undergo proton abstraction (e.g., from solvent molecules) to form a tentative EPR-active (bpy)(NMI)Cu^{II}OOH complex, which may give rise to the EPR signal in Figure 1 B (d and e). Stahl et al. postulated the reaction of (bpy)(NMI)$Cu^{II}O_2^{\cdot-}$ with another (bpy)(NMI)Cu^{I} molecule to form a binuclear $[[(bpy)(NMI)Cu]_2O_2]^{II}$ complex.[3b] Our results do not support this conclusion, because such a dimer is EPR-silent and cannot explain the observed increase of the Cu^{II} EPR signal in Figure 1 B. However, we could safely confirm the postulated coordination of bpy and NMI to Cu^{II} through their N atoms by reference EPR measurements of $Cu^{II}(OTf)_2$ in MeCN after adding bpy and NMI. In this case, a very similar EPR signal is observed, which shows superhyperfine structure (shfs) from the coupling of the Cu^{II} electron spin to the nuclear spins of three N ligands (see the Supporting Information (SI), Figure S2). Interestingly, no Cu^{II} EPR signal was observed, when $[(MeCN)_4]Cu^{I}OTf$, bpy and NMI are mixed under inert atmosphere. This clearly shows that the coordination of NMI to the (bpy)Cu^{I} complex raises its ability to reduce O_2. A decrease of the Cu^{II}/Cu^{I} reduction potential upon addition of NMI has also been found by cyclic voltammetry measurements.[3b]

When in the next step BzOH was added to the solution of (bpy)(NMI)Cu^{II} formed in situ by oxidation of (bpy)-(NMI)Cu^{I} with O_2, no changes could be observed, neither in the UV-Vis nor in the EPR spectrum [Figure 1 A (f) and 1 B (f)]. This shows clearly that (bpy)(NMI)Cu^{II} alone cannot oxidize BzOH. This happens only in the presence of TEMPO, which was added in the last step [Figure 1 A (g) and 1 B, (g)]. The EPR signal of the in situ-formed (bpy)(NMI)Cu^{II} complex decreased (compare Figure 1 B, f and g), while in the UV-Vis spectrum the MLCT band of Cu^{I} at 443 nm reappeared and the d–d band of Cu^{II} at 650 nm vanished (Figure 1 A, g). Simultaneously, catalytic activity was observed, evidenced by an IR band at 1702 cm^{-1} which is characteristic for the carbonyl group of benzaldehyde (BA).[7] The time-dependent catalytic and spectral behavior will be discussed below.

To explore explicitly the role of TEMPO, separate experiments were performed in which TEMPO has been added to a solution of the (bpy)Cu^{I} complex initially formed in MeCN. This did not change the UV-Vis spectrum, neither under inert N_2 atmosphere nor upon bubbling O_2 through the solution, and no Cu^{II} signal was observed in the EPR spectrum. This indicates that there is no interaction between TEMPO and the Cu^{I} complex. This holds also true when TEMPO is added to a solution of the (bpy)(NMI)Cu^{II} complex, whereby it does not matter whether this complex had been formed from a $Cu^{I}OTf$ or a $Cu^{II}(OTf)_2$ precursor. In both cases, the EPR and UV-Vis signals of Cu^{II} remained unchanged, which shows clearly that no direct interaction between the (bpy)(NMI)Cu^{II} complex and the TEMPO radical occurs. This is explicitly shown in Figure S3 for the MeCN solution of a (bpy)(NMI)Cu^{II} complex formed from a $Cu^{II}(OTf)_2$ precursor. The Cu^{II} signal did also not change during subsequent bubbling of oxygen through this solution. However, by in situ EPR we could clearly show that TEMPO does interact with oxygen. The signal of TEMPO broadens strongly in the presence of O_2 and this is reversible upon flushing with N_2 (Figure S4).[8] Based on this observation, we suggest that the role of TEMPO may be fixation and activation of oxygen by forming a weak TEMPO–O_2 complex. This differs from previously published mechanisms in which it was proposed that one-electron oxidation of Cu^{I} by TEMPO leads to the formation of a Cu^{II} complex.[9]

In Figure 2 the spectral behavior of the complete catalytic system is plotted as a function of time. The EPR signal of (bpy)(NMI)Cu^{II} decreased with time after adding TEMPO and BzOH and reached its minimum after 6 min (shown as starting spectrum in Figure 2 A). Afterwards it grew again up

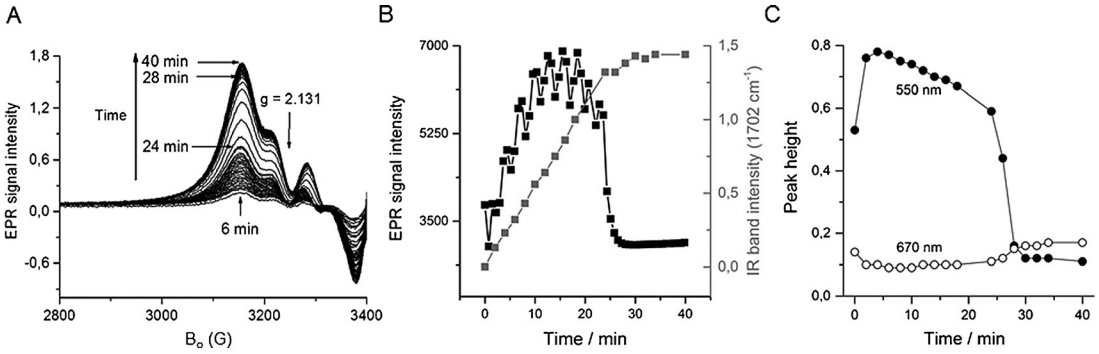

Figure 2. Time-dependent behavior of A) the Cu^{II} EPR signal, B) the intensity of the TEMPO EPR signal (obtained by double integration) and the area of the ν(C=O) ATR-IR band of benzaldehyde (corresponding ATR-IR spectra are shown in Figure S5), and C) the peak height of the UV-Vis MLCT band of (bpy)(NMI)Cu^{I} at 550 nm and the d–d band of (bpy)(NMI)Cu^{II} at 670 nm during BzOH oxidation with Cu^{I}OTf/bpy/NMI/TEMPO/O_2 in MeCN at 20 °C

to about 28 min and then remained almost constant. During the same time the ATR-IR band of BA increased and reached a plateau around 25 min indicating complete conversion of BzOH (Figure 2B). A similar trend was observed in the UV-Vis spectra. The MLCT band of (bpy)(NMI)Cu^{I} reappeared and reached its maximum after 6 min, coinciding with the minimum of the Cu^{II} EPR signal. During the next 30 min it dropped again while the maximum of the Cu^{II} EPR signal is approached (Figure 2A,C). Simultaneously, the d–d band of (bpy)Cu^{II}-NMI at 670 nm reappeared and its intensity increase after about 25 min coincides with that of the corresponding EPR spectrum. The UV-Vis spectra show an isosbestic point at 628 nm which indicates that Cu^{I} is converted to Cu^{II} without formation of an intermediate (Figure S5). The line width of the TEMPO EPR signal became narrow while its intensity increased after adding BzOH (Figures 2B and S5), indicating dissociation of the TEMPO–O_2 complex and consumption of O_2 in BzOH oxidation. When all BzOH is converted to BA after about 24 min, bubbling of O_2 into the solution leads to an accumulation of the TEMPO–O_2 complex and to a sudden broadening and intensity drop of the TEMPO signal again (Figure 2B). Interestingly, a fluctuation of line width and intensity of the TEMPO EPR signal was detected with time during conversion of BzOH which clearly indicates its involvement in the catalytic cycle by periodically forming and decomposing the TEMPO–O_2 species (Figure 2B). Note that in previous EPR measurements of quenched samples taken periodically from the reaction mixture neither such fluctuations nor any change of the TEMPO signal was detected.[3b] This shows clearly the need of true operando studies for unraveling mechanisms. When all BzOH is consumed, shape and intensity of the TEMPO signal are again similar to those before adding BzOH and the initial (bpy)(NMI)Cu^{II} complex is restored upon reoxidation of Cu^{I} (Figure 2A,B). When now another portion of BzOH is added to the system, aldehyde formation starts to continue as reflected by a further increase of its ATR-IR band (Figure S6), thus excluding catalyst deactivation and confirming complete BzOH consumption as reason for the observed spectral behavior. These results do not agree with a previous mechanism, postulating reaction of TEMPO with a (bpy)-(NMI)Cu^{II}OBz intermediate to form TEMPOH, BA, and (bpy)Cu^{I}(NMI).[3b,c,10] If this happened, the EPR signals of both TEMPO and Cu^{II} should drop just after adding BzOH because Cu^{I} and TEMPOH are EPR-silent species. From Figure 2A and B the opposite behavior is clearly evident. Nevertheless, it is obvious that the ability of the complex to shuttle between Cu^{I} and Cu^{II} might be crucial for its activity in the catalytic reaction.

To gain more information about the role of Cu^{II} we performed the same operando-spectroscopic experiments, for which a detailed description is given in section SI-A (Figure S3), starting from a $Cu^{II}(OTf)_2$ complex. Briefly, we could show that a (bpy)(NMI)Cu^{II} complex is formed, too, from the Cu^{II} precursor, yet no spectral changes of this complex upon subsequent addition of BzOH and TEMPO have been detected and no oxidation of BzOH to BA was observed under these conditions. This shows clearly that initially present Cu^{II} cannot activate O_2 in the presence of TEMPO because transfer of one electron to form a $O_2^{\bullet-}$ intermediate is not possible in this case.

Based on all results, we propose a modified reaction mechanism (Scheme 1). An in situ-formed (bpy)(NMI)Cu^{I} complex **a** (evidenced by UV-Vis spectroscopy, Figure 1A) is oxidized to (bpy)(NMI)Cu^{II} **b** with coordinated $O_2^{\bullet-}$, which—in the absence of TEMPO—might undergo further reaction, e.g., proton abstraction, to form a species seen by EPR (Figure 1B). In the presence of TEMPO, **b** is converted to **c**, evidenced by line broadening and intensity loss of the EPR signals (Figure S4B). The interaction of TEMPO with $O_2^{\bullet-}$ is well-known[11] and we have confirmed it by addition of KO_2 to a solution of TEMPO. BzOH may be deprotonated by NMI and coordinate to the Cu^{II} site (**d**). This highlights the bifunctional role of NMI as a ligand and a base and explains why two equivalents of NMI are often used in the catalytic reaction.[3a,b] $O_2^{\bullet-}$ mediates H abstraction from the α-C of the coordinated -OBz species. BA is released and the interaction between TEMPO, $O_2^{\bullet-}$, and the Cu^{II} site is broken, evidenced by decreasing line width and rising intensity of both the TEMPO and the Cu^{II} EPR signals (Figure 2). H_2O_2 is formed by reaction with H^+-NMI (**e**) and decomposed by the recreated bpy–Cu^{I} complex, which is well-known.[3b] Since the reaction has been performed in batch mode, the gradual

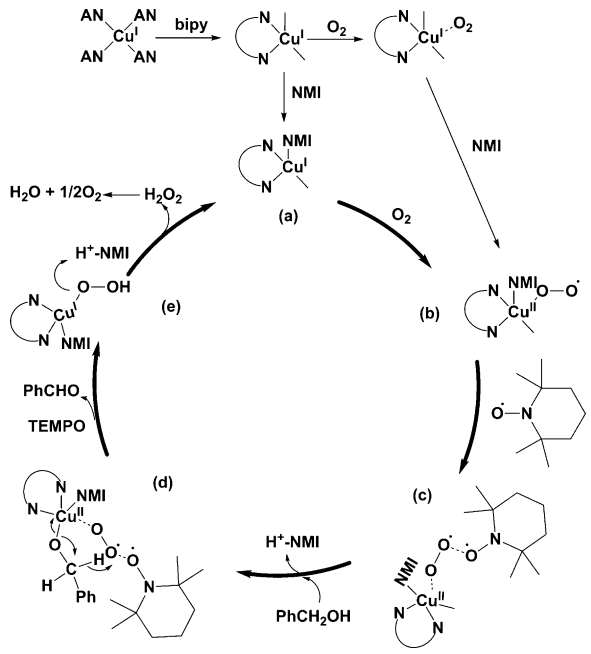

Scheme 1. Proposed reaction mechanism for alcohol oxidation over the $Cu^{I}OTf$/bpy/NMI/TEMPO/O_2 catalytic system.

decrease of BzOH in the solution leads to an accumulation of the (bpy)(NMI)Cu^{II} complex with time (Figure 1 A) which reaches its maximum at the end of the reaction when no more BzOH is available for reduction.

Note that a very similar spectral behavior has been observed when heptanol was used instead of BzOH, yet the rate of aldehyde formation as well as the rates of Cu^{I}/Cu^{II} conversion were much slower (Figure S7). This confirms previous results of cyclohexylalcohol oxidation,[3b] showing that the reaction of aliphatic alcohols is markedly slower.

In conclusion, using a new simultaneous operando-EPR/UV-Vis/ATR-IR spectroscopy setup, we obtained new mechanistic information on copper/TEMPO-catalyzed selective alcohol oxidation. We propose the formation of an active (bpy)(NM)Cu^{II}-$O_2^{\bullet-}$-TEMPO species by electron transfer from a Cu^{I} precursor, in which the role of TEMPO is activation and fixation of O_2 in the active intermediate. This deviates from previous proposals and highlights the advantage of the new coupling technique, which has general application potential also for other homogeneous catalytic reactions in which paramagnetic transition metal complexes are used as catalysts.

Experimental Section

All spectra were recorded while pumping the reaction mixture at 20 °C through a quartz flat cell placed in the cavity of the EPR spectrometer, which was equipped with fiber optical ATR-IR and UV-Vis probes as well as a capillary for O_2 admission. Details are described in section SI-F.

Keywords: alcohol oxidation · homogeneous catalysis · operando spectroscopy · TEMPO · UV/Vis spectroscopy

How to cite: *Angew. Chem. Int. Ed.* **2015**, *54*, 11791 – 11794
Angew. Chem. **2015**, *127*, 11957 – 11960

[1] a) U. Bentrup, *Chem. Soc. Rev.* **2010**, *39*, 4718 – 4730; b) A. Brückner, *Chem. Commun.* **2005**, 1761 – 1763; c) A. M. Beale, J. P. Hofmann, M. Sankar, E. M. Schrojenstein Lantman, B. M. Weckhuysen, in *Heterogeneous Catalysts for Clean Technology*, Wiley-VCH, Weinheim, **2013**, pp. 365 – 411; d) A. Vimont, F. Thibault-Starzyk, M. Daturi, *Chem. Soc. Rev.* **2010**, *39*, 4928 – 4950.
[2] K. Grabow, U. Bentrup, *ACS Catal.* **2014**, *4*, 2153 – 2164.
[3] a) B. L. Ryland, S. D. McCann, T. C. Brunold, S. S. Stahl, *J. Am. Chem. Soc.* **2014**, *136*, 12166 – 12173; b) J. M. Hoover, B. L. Ryland, S. S. Stahl, *J. Am. Chem. Soc.* **2013**, *135*, 2357 – 2367; c) J. M. Hoover, B. L. Ryland, S. S. Stahl, *ACS Catal.* **2013**, *3*, 2599 – 2605; d) S. A. Tromp, I. Matijosyte, R. A. Sheldon, I. W. C. E. Arends, G. Mul, M. T. Kreutzer, J. A. Moulijn, S. de Vries, *ChemCatChem* **2010**, *2*, 827 – 833.
[4] B. L. Ryland, S. S. Stahl, *Angew. Chem. Int. Ed.* **2014**, *53*, 8824 – 8838; *Angew. Chem.* **2014**, *126*, 8968 – 8983.
[5] a) P. L. Holland, K. R. Rodgers, W. B. Tolman, *Angew. Chem. Int. Ed.* **1999**, *38*, 1139 – 1142; *Angew. Chem.* **1999**, *111*, 1210 – 1213; b) J. E. Bol, W. L. Driessen, R. Y. N. Ho, B. Maase, L. Que, Jr., J. Reedijk, *Angew. Chem. Int. Ed. Engl.* **1997**, *36*, 998 – 1000; *Angew. Chem.* **1997**, *109*, 1022 – 1025; c) N. Kitajima, Y. Moro-oka, *Chem. Rev.* **1994**, *94*, 737 – 757.
[6] B. J. Hathaway, D. E. Billing, *Coord. Chem. Rev.* **1970**, *5*, 143 – 207.
[7] G. Socrates, *Infrared and Raman Characteristic Group Frequencies: Tables and Charts*, 3rd ed., Wiley, Hoboken, **2004**, p122.
[8] A. Moscatelli, M. F. Ottaviani, W. Adam, A. Buchachenko, S. Jockusch, N. J. Turro, *Helv. Chim. Acta* **2006**, *89*, 2441 – 2449.
[9] A. Dijksman, I. W. C. E. Arends, R. A. Sheldon, *Org. Biomol. Chem.* **2003**, *1*, 3232 – 3237.
[10] E. T. T. Kumpulainen, A. M. P. Koskinen, *Chem. Eur. J.* **2009**, *15*, 10901 – 10911.
[11] K. Takeshita, S. Okazaki, A. Itoda, *Anal. Chem.* **2013**, *85*, 6833 – 6839.

Received: May 31, 2015
Published online: July 14, 2015

